HHS Public Access

Author manuscript

Thromb Res. Author manuscript; available in PMC 2023 October 02.

Published in final edited form as:

Thromb Res. 2022 December ; 220: 131–140. doi:10.1016/j.thromres.2022.10.017.

Hyperfibrinolysis drives mechanical instabilities in a simulated model of trauma induced coagulopathy

Andrew R. Gosselin[a], **Nathan J. White**[b], **Christopher G. Bargoud**[c], **Joseph S. Hanna**[c], **Valerie Tutwiler**[a,*]

[a] Department of Biomedical Engineering, Rutgers -The State University of New Jersey, Piscataway, NJ, USA

[b] Department of Emergency Medicine, Resuscitation Engineering Science Unit, University of Washington School of Medicine, Seattle, WA, USA

[c] Department of Surgery, Rutgers-Robert Wood Johnson Medical School, New Brunswick, NJ, USA

Abstract

Introduction: Trauma induced coagulopathy (TIC) is common after severe trauma, increasing transfusion requirements and mortality among patients. TIC has several phenotypes, with primary hyperfibrinolysis being among the most lethal. We aimed to investigate the contribution of hypercoagulation, hemodilution, and fibrinolytic activation to the hyperfibrinolytic phenotype of TIC, by examining fibrin formation in a plasma-based model of TIC. We hypothesized that instabilities arising from TIC will be due primarily to increased fibrinolytic activation rather than hemodilution or tissue factor (TF) induced hypercoagulation.

Methods: The influence of TF, hemodilution, fibrinogen consumption, tissue plasminogen activator (tPA), and the antifibrinolytic tranexamic acid (TXA) on plasma clot formation and structure were examined using rheometry, optical properties, and confocal microscopy. These were then compared to plasma samples from trauma patients at risk of developing TIC.

Results: Combining TF-induced clot formation, 15 % hemodilution, fibrinogen consumption, and tPA-induced fibrinolysis, the clot characteristics and hyperfibrinolysis were consistent with primary hyperfibrinolysis. TF primarily increased fibrin polymerization rates and reduced fiber length. Hemodilution decreased clot optical density but had no significant effect on mechanical clot stiffness. TPA addition induced primary clot lysis as observed mechanically and optically.

* Corresponding author at: Department of Biomedical Engineering, Rutgers - The State University of New Jersey, 599 Taylor Road, Room 209, Piscataway, NJ 08854, USA. valerie.tutwiler@rutgers.edu (V. Tutwiler).

Declaration of competing interest

The authors have no relevant competing interests to disclose.

CRediT authorship contribution statement

VT, AG, JH, CB and NW designed experiments. AG performed experiments. VT and AG analyzed data. JH and CB attained patient consent and assisted with patient sample delivery. All authors contributed to the preparation of the manuscript.

We would like to thank John Weisel for his feedback.

Appendix A. Supplementary data

Supplementary data to this article can be found online at https://doi.org/10.1016/j.thromres.2022.10.017.

TXA restored mechanical clot formation but did not restore clot structure to control levels. Patients at risk of TIC showed increased clot formation, and lysis like that of our simulated model.

Conclusions: This simulated TIC plasma model demonstrated that fibrinolytic activation is a primary driver of instability during TIC and that clot mechanics can be restored, but clot structure remains altered with TXA treatment.

Keywords

Fibrin; Fibrinolysis; Hemorrhage; Mechanics; Blood

1. Introduction

Traumatic injuries are a significant cause of death worldwide, accounting for over 5 million deaths annually, and are the leading cause of death under 44 years old [1–4]. Of these trauma deaths, the primary cause of death is traumatic brain injury and second is exsanguination due to blood loss [5,6]. Most trauma deaths occur within the first 48 h after injury [2,5–8]. One quarter of trauma deaths are potentially survivable if effective hemorrhage control is initiated at the time of injury, and 40–64 % of these potentially survivable deaths are due in part or entirely to hemorrhage [2,9–11]. Impaired coagulation or trauma induced coagulopathy (TIC) occurs in 25 % of trauma patients and results in a 4–6-fold increase in mortality [3,10,12]. Several TIC phenotypes exist, with primary hyperfibrinolysis being associated with the greatest bleeding mortality [13,14]. Blood clots are composed of a fibrin and platelet mesh containing entrapped red blood cells and proteins. Clots must be mechanically strong enough to resist mechanical disruption from hydrodynamic forces and resistant to fibrinolytic enzymes induced during TIC. Therefore, any condition which alters fibrin formation and structure can greatly impact the ability of the blood clot to stop bleeding [15].

Early evidence indicates that multiple pathways influence the progression of TIC: tissue factor induced coagulation, hemodilution from resuscitation fluids, platelet dysfunction, endothelial dysfunction, protein C activation, fibrinogen consumption and/or modification, and hyperfibrinolysis [10]. Hyperfibrinolysis is initiated by release of tissue plasminogen activator (tPA) into the bloodstream by endothelium in response to hemorrhagic shock, leading to breakdown of fibrinogen and fibrin [16]. This increase in pro-fibrinolytic factors plays a more pronounced role in hyperfibrinolysis, than changes in the anti-fibrinolytic system [12]. Primary hyperfibrinolysis is a rapid and intense hyperfibrinolytic state that occurs in a subset of trauma patients and if not detected early can result in mortality rates of 60–100 % [17–20]. Fibrinolysis is associated with decreased clot strength in TIC patients which are ~40 % weaker than normal clots [21,22]. Rapid loss of fibrinogen due to depletion from hemorrhage, coagulation consumption, and dilution from resuscitation fluids also contributes to coagulopathy and has been associated with mortality and coagulopathy after trauma [23]. Therefore, determining how these important biochemical changes related to fibrinogen and fibrin formation influence clot structure and mechanical stability is critical to informing the development of novel treatments.

In cases of severe trauma, hyperactivation of the coagulation system leading to consumption of fibrinogen and coagulation factors, is often coupled with hyperfibrinolysis [24]. On average, hyperfibrinolytic patients have a 10–15 % reduced hemoglobin level and 15–20 % decreased platelet counts compared to other trauma populations [18]. As well as elevated tPA levels compared to healthy patients, 139pM vs 32pM, and robust increases in thrombin generation, 122.2 nM vs 86.3 nM in healthy controls [12,25]. Using an in-vitro whole blood model, Kostousov et al. determined that whole blood diluted 15 %, initiated with 45pM human recombinant TF (Recombiplastin, Plastinex, BioData Corporation, MA, USA) supplemented with 3.3 mM tPA (225 ng/mL) recreated a primary hyperfibrinolysis clot formation pattern like that seen in TIC patients when measured using thrombelastography [26]. They also reported that fibrinolysis could be inhibited by TXA [26]. However, the use of a whole blood model limits the ability to isolate and examine fibrin-specific structural and mechanical changes attributable to TIC. We used rheometry, turbidity, and confocal microscopy to investigate how the individual and combined basic components of TIC affect fibrin clot structure and formation using a plasma model of simulated TIC (STIC). This model will be used as an ex-vivo model of TIC to investigate the efficacy of new therapies and their combinatorial effects on coagulopathy. We will compare this model of TIC and its components to plasma from trauma patients at risk for TIC.

2. Materials and methods

2.1. Sample preparation

Citrated, de-identified human plasma was obtained from 25 donors from discarded blood bank donation, following informed consent of healthy subjects in accordance with the University of Pennsylvania and State University of New York Stony Brook Blood Blank guidelines. Platelet poor plasma (PPP) was fractionated by plasmapheresis. PPP was diluted with citrate phosphate dextrose anticoagulant, to a final concentration of four parts PPP and one part citrate phosphate dextrose. PPP was frozen within 8 h at −65 °C following blood bank donation, once all the plasma samples were collected, they were thawed once, pooled, filtered, and then refrozen at −80 °C. The fibrinogen concentration in the final PPP solution was 2.7 ± 0.2 mg/mL determined by spectrophotometric analysis at the University of Pennsylvania. After initiation of clotting in an excess of thrombin (100 U/mL) the clot was washed and dissolved in 0.25 M NaOH. The concentration was analyzed in triplicate from absorbance at 280 nm wavelength compared to a known standard absorbance. For each testing method, pooled PPP was warmed to 37 °C, with clotting initiated by 20 mM calcium chloride ($CaCl_2$) (final concentration, Sigma-Aldrich), and 0.2 unit/mL thrombin (final concentration, Sigma-Aldrich). Immediately after the addition of clotting agents, the plasma was used in rheometer testing, confocal imaging, or turbidity testing.

2.2. Plasma fibrinogen depletion

PPP was supplemented with 17uM batroxobin in methanol (final concentration) and 20 mM $CaCl_2$ (final concentration) and left to clot for 2 h at 37 °C then centrifuged at 4000 rpm for 15 min and supernatant was removed and stored at 4 °C for 48 h. The plasma was then centrifuged again at the same parameters to remove any leftover fibrin, stored at −80 °C until

needed as fibrinogen depleted plasma and checked to ensure no leftover batroxobin or $CaCl_2$ was left.

2.3. Rheometer mechanical testing

A Malvern Kinexus Ultra rheometer (Netzsch, Selb, Germany) was used to analyze the viscoelastic properties of thawed plasma. Samples were activated with $CaCl_2$ and thrombin, mixed, and quickly transferred to the rheometer lower geometry. An oscillation strain test was performed on 490 uL samples, at 7.8 Hz and 4.29 % shear strain using a 40-mm parallel plate, a 0.35 mm working gap and 2 s sampling rate for 1 h. The main information collected and quantified was the Storage (G'), Loss (G") moduli, and tan delta (G"/G'). These correspond to the stored energy, dissipated energy and the ratio between storage and loss moduli of the plasma clot as it polymerizes. Polymerization rate was taken as the rate of G' increase over time between 1 % to 40 % of the maximum G' to focus on the polymerization stage of the process and remove the effect of drying on analysis (Fig. S1).

2.4. Optical turbidity testing

A Molecular Devices Spectramax Plus (Molecular Devices, San Jose, California) plate reader was used to analyze the optical properties of thawed (37 °C) plasma. Plasma was pooled from at least 25 donors thereby mitigating differences in baseline optical density. Turbidity measured the opacity of the solution as the plasma clotted and lysed. Samples were activated as described above and transferred to a clear bottom 96 well plate, replicates were placed side by side, and further samples were placed in the proceeding rows. Wells immediately surrounding samples were filled with 200uL water to prevent drying of clots. The optical density was measured every 15 s for 90 min, at 405 nm wavelength and 37 °C. The optical density was normalized to 0 in all experiments as changes in plasma additions may alter the starting opacity of samples. Polymerization rate was taken as the rate increase over time between 20 % to 70 % of the maximum optical density.

2.5. Confocal microscopy

A Zeiss LSM 710 Confocal microscope (Zeiss, Oberkochen, Germany) was used to image the control, STIC and STIC+TXA plasma samples. These clots were prepared in 1.5 mL Eppendorf tubes, 1 % of the plasma volume was replaced with 1.5 mg/mL Alexa Fluor 488–labeled fibrinogen (Thermo Fisher Scientific, USA). Clotting was initiated as described above and samples were added to a clear bottom borosilicate glass 24 well plate and transferred to the confocal stage. Plasma samples were imaged using 2048 × 2048 resolution, 40 × water immersion objective, 1.20 numerical aperture, with an image area of 213 × 213 micrometers. Image settings were kept constant across all images and clot samples. Samples were imaged for at least 60 min and were run in triplicate with single plane images taken of each sample then analyzed for the following criteria.

2.6. Image analysis

Image analysis was completed using ImageJ software and Matlab Simulink R2020a. The images were taken as .czi files from the Zeiss Zen software, gray scaled and exported as a .tif file for use in Matlab. To calculate % fibrin density the .tif files were uploaded

to Matlab, thresholded and binarized using Otsu's method to remove background, then particles smaller than 5 pixels were removed. Four areas from each image were selected and analyzed to calculate fibrin density. Fiber length and pore size were measured by manually using ImageJ and calculated from the average of 20 fibers and pores for each sample time point from the 2D image.

2.7. Patient sample collection

Blood samples were collected from patients admitted to the Robert Wood Johnson University Hospital Emergency Department following informed consent under approval by the Rutgers's University Institutional Review Board. Inclusion criteria are as follows: patients 18 years and older, with any of the following: prehospital endotracheal intubation or assisted ventilation, with a respiratory rate < 10 or > 29 breaths per minute. Patients aged 18–64 with systolic blood pressure < 90 mmHg or sustained heart rate > 120 or < 40 beats per minute. For ages >64 a systolic blood pressure <100 mmHg or sustained heart rate >120 or < 40 beats per minute. Any patients with pre-hospital transfusion to maintain vital signs, with active hemorrhage, with glasgow coma score < 9, penetrating injury to the head, neck, torso, or extremities proximal to the elbow or knee or patients with crushed, amputated, degloved, mangled or pulseless extremities proximal to the wrist or ankle. Exclusion criteria include patients from which a sample could not be obtained prior to death, younger than 18 years of age, weigh <110 pounds, women who were pregnant, patients on systemic anticoagulation or antiplatelet drugs at the time of injury, any patient transferred from an outside institution, or any patient presenting with bleeding diathesis or hereditary coagulopathy at baseline.

2.8. Patient sample preparation

Blood was collected into 3.2 % sodium citrate (9:1, *v*/v) from patients after arrival to the hospital. Blood was stored at 4 °C for a maximum of 16 h before plasma was isolated. Plasma was isolated by centrifugation at 2400 rpm for 10 min and stored at −80 °C until subjected to mechanical and optical turbidity testing. After blood was collected and processed for storage it was determined if the patient fit exclusion/inclusion criteria, and then informed consent was obtained from the patient or a surrogate as per IRB approval from the Rutgers University Institutional Review Board. If inclusion criteria were not met, or consent was not obtained, the blood or plasma sample was disposed of.

2.9. Patient rheometer mechanical testing

Patient samples were tested with the same Malvern Kinexus Ultra Rheometer after activation with 20 mM $CaCl_2$ and 0.2 U/mL thrombin. An oscillation strain test was performed with a 20 mm parallel plate on 120uL samples, at 7.8 Hz and 4.29 % shear strain, a 0.35 mm working gap and 2 s sampling rate for 1 h.

2.10. Patient optical turbidity testing

Patient samples were tested on a Molecular Devices Spectramax Plus to analyze the optical properties of thawed (37 °C) plasma. All testing parameters and activation conditions were kept the same as those used for the PPP samples in our STIC model.

2.11. Patient tissue plasminogen activator ELISA

Tissue plasminogen activator (tPA) concentration in human plasma was measured using the Abcam tPA human ELISA kit (ab108914, Abcam). Following the manufacturer's instructions tPA was measured using a Molecular Devices Spectramax Plus (Molecular Devices, San Jose, California) plate reader, measuring absorbance at 450 nm wavelength and interpolation from the standard curve. All samples were run in duplicate.

2.12. Statistical analysis

Statistical analyses were performed using GraphPad Prism 9.0. One-way and two-way analysis of variance (ANOVA) were used to compare differences between data sets, followed by a Tukey test to find statistical significance between groups. All data are represented as mean ± standard error of the mean unless otherwise noted for at least three replicates. Lack of significant differences between samples is indicated by no bar above the samples graphed.

3. Results

3.1. Simulated trauma induced coagulopathy (STIC) model

To create a plasma-based model of the dilutional coagulopathy model first described by Kostousov et al. [26], PPP was diluted with 15 % saline (Sigma-Aldrich) by volume to model fibrinogen dilution, 3.3 mM tPA (Sigma-Aldrich, MO, USA), to initiate fibrinolysis, and 45 pM TF, inducing hypercoagulability. STIC samples had 9–16-fold faster fibrin polymerization rates than controls across testing methods ($p < 0.001$, Fig. 1E, F) leading to a higher storage modulus and optical density at 600 s, (103 Pa vs 7.4 Pa, $p < 0.005$, Fig. 1C, D). The loss modulus (viscous component) was similar, and the tan delta decreased as clots stiffened (Fig. S2A, B). Along with faster plasma clot formation, STIC samples showed disintegration of the fibrin network by 1500 s as determined by the loss of viscoelastic and optical properties (Fig. 1A, B). Similar behavior was observed using confocal microscopy, where the STIC clot formed much faster than the control with the eventual lysis of all fibrin fibers after 30 min ($p < 0.001$, Fig. 2A). Control clots showed less dense networks, with longer fibrin fibers and larger pore sizes in comparison to STIC samples, indicating further structural changes due to TIC which may further impact clot stability ($p < 0.001$, Fig. 2B–D). To determine how hyperactivation, hemodilution, and hyperfibrinolysis, individually influence the clotting kinetics in STIC samples, we systematically varied these components.

3.2. The effect of hyperactivation on plasma clot properties

Alone, TF addition increased fibrin polymerization rate 9–15-fold, resembling STIC samples, leading to a higher initial storage modulus and optical density 600 s after plasma clot formation ($p < 0.001$, Fig. 3). TF addition did not alter the final storage modulus, but there was a decrease in the final optical density of PPP with TF ($p < 0.001$, Fig. 3C, D). To further study the impact of hypercoagulation on clot properties the concentration of TF added was doubled to 90pM (2× TF) and analyzed similarly. Testing showed a similar increase in polymerization rate between TF and 2× TF samples, with 2× TF showing similar maximum storage modulus and optical density compared to controls (Fig. S4).

3.3. The effect of fibrinolysis on plasma clot properties

PPP supplemented with 3.3 mM tPA did not alter the initial storage modulus, optical density, or polymerization rates compared to controls up to 300–600 s (Fig. 3A, B). However, tPA samples quickly lysed after this period, leading to a reduced maximum storage modulus and optical density across tests (Fig. 3A–D). Across methods, fibrinolysis rate was faster in STIC samples than PPP with tPA alone ($p < 0.005$, Fig. S5). However, the overall time to complete lysis was similar in STIC and tPA samples in mechanical tests, while turbidity showed STIC samples took longer to fully lyse than tPA samples (Fig. 3A, B). To further study the impact of fibrinolysis on clot formation, the concentration of tPA added was doubled to 6.6 mM (2× tPA) and analyzed similarly. Increasing tPA concentration led to faster fibrinolysis and time to complete lysis but did not change the polymerization rate, supporting the relationship between increasing fibrinolysis and instability (Fig. S4, S5). Mechanical and optical testing showed similar fibrinolysis rates at both the tPA and 2× tPA concentrations, leading to complete lysis after 1500 s (Fig. S5).

3.4. The effect of hemodilution on plasma clot properties

The 15 % dilution with saline did not change fibrin polymerization rate, or storage modulus during the period tested (Fig. 3). This dilution did lead to a lower final optical density than the control, like the reduction seen at 600 s in STIC samples (Fig. 3B, D). Further dilutions were tested at 30 %, 45 %, and 60 % PPP dilution with saline (2.7–1.1 mg/mL fibrinogen). This dilutes all factors present in the PPP and led to a clear decrease in how visually opaque the sample was prior to activation, referred to as “baseline turbidity”. Increasing saline dilution did not greatly reduce final storage modulus but did lead to significant decreases in optical density and decreasing trend in polymerization rate ($p < 0.05$, Fig. S6).

3.5. The effect of fibrinogen consumption on plasma clot properties

To further investigate alternative components of TIC we investigated the impact of fibrinogen specific consumption on plasma clot properties instead of saline dilution which diluted all coagulation factors present. Fibrinogen consumption was modeled by diluting the PPP with fibrinogen depleted plasma prior to activation for optical testing. Dilutions were similarly tested from 0 %–60 % dilution (2.7–1.1 mg/mL fibrinogen) (Fig. S7). Fibrinogen depleted plasma dilution led to no baseline turbidity changes like those seen in saline diluted samples. Increasing fibrinogen depleted plasma dilution led to decreasing final optical density and reduced polymerization rate ($p < 0.05$, Fig. S7B, C). Optical testing was used to compare saline and fibrinogen depleted plasma dilution. Polymerization rate was faster in fibrinogen depleted plasma diluted plasma at 15 % dilution but did not affect rates with further dilution ($p < 0.001$, Fig. S7E). PPP diluted with depleted plasma had consistently higher final optical density than similar dilutions with saline, except at the highest dilution at 60 % ($p < 0.005$, Fig. S7D). The STIC model was repeated but diluted with 15 % fibrinogen depleted plasma to compare a consumptive TIC to a dilutional TIC phenotype. Optical testing showed that fibrin polymerization was 8-times faster in depleted STIC samples compared to the control, like saline diluted STIC ($p < 0.001$, Fig. 4C). Depleted and saline diluted STIC samples showed similar optical density at all time points

(Fig. 4). Both TIC models, dilutional and consumptive, showed complete fibrin structure degradation by 1800–2000s as well as similar fibrinolysis rates (Fig. 4, S5).

3.6. Comparison of clinical samples and STIC components

To assess the clinical relevance of our findings we compared components of our experimental model with samples from individual patients admitted to the emergency room following traumatic injury. As shown in Table 1, Patient #1 had low fibrinogen levels (0.38 mg/mL) and high D-dimer levels (128,000 ng/mL), as well as increased tPA concentration (14.7 ng/mL) indicating significant fibrinolysis was occurring (Fig. 5G). This patient sample showed similar trends in stiffness and OD measurements as compared to the control samples with tissue plasminogen activator (tPA) added to simulate coagulopathic fibrinolysis (Fig. 5A–D). Likewise Patient #2 had a hypercoagulant phenotype and presented with high levels of fibrinogen (4.48 mg/mL), moderate D-dimer levels (7370 ng/mL) and moderate amounts of tPA (7.5 ng/mL) (Fig. 5). This sample showed similar trends in OD and stiffness as the control samples hyperactivated with TF in our model, however with slight fibrinolysis present (Fig. 5). These findings indicate that our plasma-based in vitro model can simulate changes that occur in clot formation/degradation and mechanics following traumatic injury. The comparison to patient samples requires further examination going forward.

3.7. The Impact of Tranexamic Acid Administration on STIC Plasma

To confirm that hyperfibrinolysis drives the instability seen in STIC samples, we added 10 mM tranexamic acid (TXA) to STIC samples (STIC+TXA) to inhibit fibrinolysis. This concentration was sufficient to prevent 98 % of fibrinolysis in previous literature and inhibit the high level of tPA used in this STIC model [27]. STIC and STIC+TXA had similar polymerization rates, 7–16 times faster than controls, as well as similar stiffness and optical density at 600 s ($p < 0.01$, Fig. 6). However, after 1200 s STIC samples quickly started to lyse where STIC+TXA maintained its structure and stability after this point (Fig. 6). This was supported with confocal imaging which showed STIC+TXA samples had similar fiber density, fiber length and pore size as STIC samples at each time point, prior to STIC sample lysis (Fig. 2A). To determine the impact of the timing of TXA administration, we added 8uL of TXA (10 mM final concentration) to the STIC sample at 5 min, 10 min or 15 min and compared these timepoints to the control, STIC and STIC+TXA sample (Fig. S8). Increasing time to TXA addition led to increased lysis and decreased final optical density (Fig. S8B–D). As post traumatic thromboembolism after TXA administration is of concern in patients we determined if TXA influenced other aspects of clot formation [28,29]. The STIC+TXA sample was repeated while excluding tPA from the sample (STIC+TXA no tPA) but there were no significant differences in any property in comparison to the STIC+TXA sample (Fig. S9).

4. Discussion

The purpose of our study was to examine how individual contributors to TIC affect clot formation in a simulated model of primary hyperfibrinolysis. We found that enzymatic fibrinolytic activation by tPA was the dominant driving cause of mechanical instability in our model. Enzymatic dissolution of the fibrin network witnessed on confocal examination

was also the dominant structural change that coincided with mechanical and optical lysis patterns. In addition, changes specifically of fibrinogen concentration were the primary cause of changes in fibrin clot formation during hemodilution. These results suggest that changes in fibrinogen concentration, its polymerization to fibrin, and irreversible dissolution of fibrin are of the utmost importance to TIC. In addition, we found turbidity to be more sensitive than mechanical testing to detect TIC.

4.1. Fibrinolytic activation accounts for instability in simulated TIC

Hyperfibrinolysis is a maladaptive overactivation of the plasma fibrinolytic system and is characterized by a rapid decrease in clot stiffness. Hyperfibrinolysis can be identified by a terminal decrease of clot firmness using viscoelastic assays or by levels of fibrin degradation products such as D-Dimer [16,30]. This was modeled in our study with the addition of tPA to spur the activation of plasmin and lyse the plasma clot. Addition of tPA, both alone and in the STIC model, led to a drastic reduction in clot stiffness and optical density after clot formation began (Fig. 3). The addition of tPA prevented the clots from reaching their maximum storage modulus or optical density across testing methods (Fig. 3). This indicates that fibrinolysis both prevents the formation of a stable clot and induces degradation of formed clots, pointing to a prominent role in the loss of stability seen in TIC as opposed to hemodilution, consumption or hyperactivation which had limited impact on clot stability. To ensure that fibrinolysis was the main contributor to this clot breakdown, we tested the use of TXA, a synthetic antifibrinolytic to prevent this fibrinolysis. TXA is used to treat fibrinolysis to prevent traumatic and perioperative bleeding by preventing the conversion of plasminogen to plasmin, preventing fibrin degradation [31–34]. Testing showed that addition of TXA to the STIC sample prevented fibrinolysis from occurring but did not affect other coagulation properties (Figs. 2, 6). STIC+TXA samples had similar final storage modulus as controls, thought it had a similar fibrin structure as STIC prior to STIC sample lysis, indicating that the altered fibrin structure did not greatly impact plasma clot stiffness (Fig. 6C). However, optical testing showed that STIC+TXA had a significantly lower maximum optical density than controls, like that of STIC, indicating a difference in the ability of tests to detect sample differences (Fig. 6D). Further, increasing time to TXA administration led to increased lysis and reduced optical density (Fig. S8B, C). The addition of TXA at later time points did stop lysis from completely degrading the sample, however it did not bring the sample back to the control or STIC+TXA final optical density (Fig. S8A). Though the TXA addition at later time points did not restore clot stability, it presents the opportunity for future tests to pair TXA administration with other therapeutics such as cryoprecipitate, freeze dried fibrinogen, or fibrinogen concentrate to enable clot formation after lysis is inhibited.

4.2. Fibrinogen is the primary contributor to clot stiffness and turbidity in STIC plasma

Fibrinogen and fibrin are essential for maintaining hemostasis and are essential to ensure that patients maintain adequate concentrations after trauma as patients with low fibrinogen concentrations (< 1 mg/mL) show drastically increased mortality [35,36]. These low levels can occur for several reasons, blood loss due to hemorrhage, hemodilution due to resuscitation fluids, and fibrinogen consumption from coagulation [37]. The loss of fibrinogen is a key mechanism indicated in the development of TIC, preventing the formation of a stable clot [23]. To model the effect of dilution from resuscitation fluids,

we analyzed plasma samples at varying dilutions with saline, from 2.7 to 1.1 mg/mL. Rheological testing showed increasing saline dilution, lead to slight reductions in final elastic modulus (Fig. S6). Whereas turbidity analysis showed larger decreases in the final optical density as fibrinogen concentration decreased (Figs. S6, S7). Showing clear differences in the ability of tests to detect differences in clot changes. Since they are different types of tests, this is expected, but this indicates that the use of multiple tests could provide crucial information where one test cannot. This method emulates the dilution aspect of coagulopathy, but it is limited in that the saline dilution reduces fibrinogen levels as well as other factors present in the plasma. To assess fibrinogen specific dilution, we diluted PPP with fibrinogen depleted plasma to specifically reduce the overall fibrinogen levels. Analysis showed a clear reduction in final optical density and fibrin polymerization rate as fibrinogen depleted plasma dilution increased (Fig. S7B, C). There were several differences between dilution with saline, and with fibrinogen depleted plasma. Saline dilution showed a larger decrease on the final optical density of plasma, compared to fibrinogen depleted plasma dilution except for the 60 % dilution ($p < 0.005$, Fig. S7). Indicating the dilutional impact of crystalloids or resuscitative fluids would have a more drastic impact on clot formation than the effect of fibrinogen consumption alone. By selectively reducing the fibrinogen concentration of the PPP we were able to determine that reduced fibrinogen concentration is the main cause of decreasing optical density when diluting the plasma. This improves our understanding of how different TIC phenotypes, dilutional vs consumptive, can alter the structure of a blood clot and impair hemostasis.

4.3. Optical testing methods are more sensitive than mechanical in STIC plasma

Thromboelastography (TEG) and thromboelastometry (ROTEM) have been used to supplement traditional coagulation tests like PT, aPTT, and INR, as they provide additional information on the coagulation process and fibrinolysis. These tests evaluate the presence of hyperfibrinolysis and help to guide transfusions to get early control of bleeding after trauma. However as has been shown in this study, though viscoelastic tests can provide key information in the formation and lysis of a clot, there exists deficiencies in their ability to detect differences in the fibrinogen concentration of samples caused by dilution from fluids. Rheological testing required much larger dilutions than turbidity testing to see changes in the final storage modulus of saline diluted samples (Fig. S6). Furthermore, key changes were present between STIC+TXA and control samples, seen in turbidity and confocal testing as reduced maximum OD and altered fibrin structure. However, these changes did not translate to a substantial change in maximum storage modulus (Fig. 6). These examples point towards the limited effectiveness of using one testing method as an aid to patient therapeutic delivery, indicating the need of multiple or improved tests to specifically determine the differences in clots.

4.4. Study strengths and limitations

The development of this STIC model helps to show how combinatorial analysis methods can be used to elucidate TIC related pathways to develop targeted treatments while also providing a platform for testing treatments. Moreover, it points to the importance of developing diagnostic tools that can distinguish between aspects of TIC. It is important to note that this is a simulated model of coagulopathy, and therefore the components of

the model are tightly controlled and there are numerous factors that are not included in this model that would be present during coagulopathy in-vivo. Going forward, we plan to overcome these limitations by developing our model further to include platelet rich plasma and whole blood to determine how the presence of cells influence the mechanisms described here. As well as including other factors which are present during TIC such as acidemia, hypothermia, and the interplay between each factor, determining how each contributes to poor clot formation in TIC. For example, activated platelets have been shown to play a role in the early phases of TIC [4,9]. Platelets are integral to the coagulation process, they both contract the fibrin mesh network and produce extra tissue factor to speed up thrombin production [4,9]. In the future, incorporating platelets into this plasma model can be used to probe their contribution to key aspects of the coagulation cascade post trauma. This corresponds to our findings related to the role of increased tissue factor and the related impact on coagulation rate in the onset of clot formation and suggests that the inclusion of platelets can shed further light on these TIC mechanisms. Interestingly, our results show that these early changes in clot formation have a limited impact on the disintegration of the clot, as shown by the similarity between degradation rates of STIC samples and those with tPA alone (Fig. 3, S4). As platelets release a magnitude of factors it will be useful to examine if other factors contribute to regulating the rate of fibrinolysis. These additions will go into further improving the understanding of the underlying mechanisms of TIC phenotypes to develop patient-specific diagnostics and therapeutics.

Supplementary Material

Refer to Web version on PubMed Central for supplementary material.

Funding

This work was supported by the National Institutes of Health (NIH) [NIH R00HL148646–01 (V.T.)].

Abbreviations:

TIC	Trauma Induced Coagulopathy
TF	Tissue Factor
tPA	tissue plasminogen activator
TXA	Tranexamic Acid
STIC	Simulated Trauma Induced Coagulopathy
PPP	Platelet Poor Plasma
IRB	Institutional Review Board
WBC	White Blood Cell
RBC	Red Blood Cell
PTT	Partial Thromboplastin Time

PT	Prothrombin Time
INR	International Normalized Ratio
FBG	Fibrinogen
FDP	Fibrinogen Depleted Plasma

References

[1]. Sakran JV, Greer SE, Werlin E, McCunn M, Care of the injured worldwide: trauma still the neglected disease of modern society, Scand. J. Trauma Resusc. Emerg. Med. 20 (2012) 64. [PubMed: 22980446]

[2]. Eastridge BJ, Holcomb JB, Shackelford S, Outcomes of traumatic hemorrhagic shock and the epidemiology of preventable death from injury, Transfusion 59 (S2) (2019) 1423–1428. [PubMed: 30980749]

[3]. Maegele M, Acute traumatic coagulopathy: incidence, risk stratification and therapeutic options, World J Emerg Med 1 (1) (2010) 12–21. [PubMed: 25214935]

[4]. Moore EE, Moore HB, Kornblith LZ, Neal MD, Hoffman M, Mutch NJ, et al. , Trauma-induced coagulopathy, Nat Rev Dis Primers 7 (1) (2021) 30. [PubMed: 33927200]

[5]. Sobrino J, Shafi S, Timing and causes of death after injuries, Proc (Bayl Univ Med Cent). 26 (2) (2013) 120–123. [PubMed: 23543966]

[6]. Sauaia A, Moore FA, Moore EE, Moser KS, Brennan R, Read RA, et al. , Epidemiology of trauma deaths: a reassessment, J. Trauma 38 (2) (1995) 185–193. [PubMed: 7869433]

[7]. Rogers FB, Shackford SR, Hoyt DB, Camp L, Osler TM, Mackersie RC, et al. , Trauma deaths in a mature urban vs rural trauma system. A comparison, Arch. Surg. 132 (4) (1997) 376–381, discussion 81–2. [PubMed: 9108758]

[8]. Scope A, Farkash U, Lynn M, Abargel A, Eldad A, Mortality epidemiology in low-intensity warfare: Israel defense forces' experience, Injury 32 (1) (2001) 1–3. [PubMed: 11164393]

[9]. White NJ, Newton JC, Martin EJ, Mohammed BM, Contaifer D Jr., Bostic JL, et al. , Clot formation is associated with fibrinogen and platelet forces in a cohort of severely injured emergency department trauma patients, Shock 44 (Suppl 1) (2015) 39–44. [PubMed: 25643013]

[10]. Cardenas JC, Wade CE, Holcomb JB, Mechanisms of trauma-induced coagulopathy, Curr. Opin. Hematol. 21 (5) (2014) 404–409. [PubMed: 25010798]

[11]. Teixeira PG, Inaba K, Hadjizacharia P, Brown C, Salim A, Rhee P, et al. , Preventable or potentially preventable mortality at a mature trauma center, J Trauma 63 (6) (2007) 1338–1346, discussion 46–7. [PubMed: 18212658]

[12]. Chapman MP, Moore EE, Moore HB, Gonzalez E, Gamboni F, Chandler JG, et al. , Overwhelming tPA release, not PAI-1 degradation, is responsible for hyperfibrinolysis in severely injured trauma patients, J. Trauma Acute Care Surg. 80 (1) (2016) 16–23, discussion-5. [PubMed: 26491796]

[13]. Kashuk JL, Moore EE, Sawyer M, Wohlauer M, Pezold M, Barnett C, et al. , Primary fibrinolysis is integral in the pathogenesis of the acute coagulopathy of trauma, Ann Surg 252 (3) (2010) 434–442, discussion 43–4. [PubMed: 20739843]

[14]. Taylor JR 3rd, Fox EE, Holcomb JB, Rizoli S, Inaba K, Schreiber MA, et al. , The hyperfibrinolytic phenotype is the most lethal and resource intense presentation of fibrinolysis in massive transfusion patients, J. Trauma Acute Care Surg. 84 (1) (2018) 25–30. [PubMed: 28914713]

[15]. Litvinov RI, Weisel JW, Fibrin mechanical properties and their structural origins, Matrix Biol. 60–61 (2017) 110–123.

[16]. Hayakawa M, Maekawa K, Kushimoto S, Kato H, Sasaki J, Ogura H, et al. , Hyperfibrinolysis in severe isolated traumatic brain injury may occur without tissue hypoperfusion: a retrospective observational multicentre study, Crit. Care 21 (1) (2017) 222. [PubMed: 28830477]

[17]. Schochl H, Frietsch T, Pavelka M, Jambor C, Hyperfibrinolysis after major trauma: differential diagnosis of lysis patterns and prognostic value of thrombelastometry, J. Trauma 67 (1) (2009) 125–131. [PubMed: 19590321]

[18]. Cotton BA, Harvin JA, Kostousouv V, Minei KM, Radwan ZA, Schochl H, et al. , Hyperfibrinolysis at admission is an uncommon but highly lethal event associated with shock and prehospital fluid administration, J. Trauma Acute Care Surg. 73 (2) (2012) 365–370, discussion 70. [PubMed: 22846941]

[19]. Levrat A, Gros A, Rugeri L, Inaba K, Floccard B, Negrier C, et al. , Evaluation of rotation thrombelastography for the diagnosis of hyperfibrinolysis in trauma patients, Br. J. Anaesth. 100 (6) (2008) 792–797. [PubMed: 18440953]

[20]. Banerjee A, Silliman CC, Moore EE, Dzieciatkowska M, Kelher M, Sauaia A, et al. , Systemic hyperfibrinolysis after trauma: a pilot study of targeted proteomic analysis of superposed mechanisms in patient plasma, J. Trauma Acute Care Surg. 84 (6) (2018) 929–938. [PubMed: 29554044]

[21]. Nystrup KB, Windelov NA, Thomsen AB, Johansson PI, Reduced clot strength upon admission, evaluated by thrombelastography (TEG), in trauma patients is independently associated with increased 30-day mortality, Scand J Trauma Resusc Emerg Med. 19 (2011) 52. [PubMed: 21955460]

[22]. Davenport R, Manson J, De'Ath H, Platton S, Coates A, Allard S, et al. , Functional definition and characterization of acute traumatic coagulopathy, Crit. Care Med. 39 (12) (2011) 2652–2658. [PubMed: 21765358]

[23]. White NJ, Chien D, Hess JR, Effect of emergency department fibrinogen testing on survival of trauma patients receiving blood transfusions, Blood Coagul. Fibrinolysis 31 (6) (2020) 372–376. [PubMed: 32618590]

[24]. Hayakawa M, Pathophysiology of trauma-induced coagulopathy: disseminated intravascular coagulation with the fibrinolytic phenotype, J. Intensive Care 5 (2017) 14. [PubMed: 28289544]

[25]. Coleman JR, Moore EE, Samuels JM, Cohen MJ, Silliman CC, Ghasabyan A, et al. , Whole blood thrombin generation in severely injured patients requiring massive transfusion, J. Am. Coll. Surg. 232 (5) (2021) 709–716. [PubMed: 33548446]

[26]. Kostousov V, Wang YW, Cotton BA, Wade CE, Holcomb JB, Matijevic N, Influence of resuscitation fluids, fresh frozen plasma and antifibrinolytics on fibrinolysis in a thrombelastography-based, in-vitro, whole-blood model, Blood Coagul. Fibrinolysis 24 (5) (2013) 489–497. [PubMed: 23406662]

[27]. Picetti R, Shakur-Still H, Medcalf RL, Standing JF, Roberts I, What concentration of tranexamic acid is needed to inhibit fibrinolysis? A systematic review of pharmacodynamics studies, Blood Coagul. Fibrinolysis 30 (1) (2019) 1–10. [PubMed: 30585835]

[28]. Myers SP, Kutcher ME, Rosengart MR, Sperry JL, Peitzman AB, Brown JB, et al. , Tranexamic acid administration is associated with an increased risk of posttraumatic venous thromboembolism, J. Trauma Acute Care Surg. 86 (1) (2019) 20–27. [PubMed: 30239375]

[29]. Meaidi A, Morch L, Torp-Pedersen C, Lidegaard O, Oral tranexamic acid and thrombosis risk in women, EClinicalMedicine 35 (2021), 100882. [PubMed: 34124632]

[30]. Hayakawa M, Maekawa K, Kushimoto S, et al. , High D-dimer levels predict a poor outcome in patients with severe trauma, even with high fibrinogen levels on arrival: a multicenter retrospective study, SHOCK 45 (3) (2016) 308–314, 10.1097/SHK.0000000000000542. [PubMed: 26882403]

[31]. Pabinger I, Fries D, Schochl H, Streif W, Toller W, Tranexamic acid for treatment and prophylaxis of bleeding and hyperfibrinolysis, Wien. Klin. Wochenschr. 129 (9–10) (2017) 303–316. [PubMed: 28432428]

[32]. Wu X, Benov A, Darlington DN, Keesee JD, Liu B, Cap AP, Effect of tranexamic acid administration on acute traumatic coagulopathy in rats with polytrauma and hemorrhage, PLoS One. 14 (10) (2019), e0223406. [PubMed: 31581265]

[33]. McCormack PL, Tranexamic acid: a review of its use in the treatment of hyperfibrinolysis, Drugs 72 (5) (2012) 585–617. [PubMed: 22397329]

[34]. Godier A, Roberts I, Hunt BJ, Tranexamic acid: less bleeding and less thrombosis? Crit. Care 16 (3) (2012) 135. [PubMed: 22748073]

[35]. Inaba K, Karamanos E, Lustenberger T, Schochl H, Shulman I, Nelson J, et al. , Impact of fibrinogen levels on outcomes after acute injury in patients requiring a massive transfusion, J. Am. Coll. Surg. 216 (2) (2013) 290–297. [PubMed: 23211116]

[36]. Hagemo JS, Stanworth S, Juffermans NP, Brohi K, Cohen M, Johansson PI, et al. , Prevalence, predictors and outcome of hypofibrinogenaemia in trauma: a multicentre observational study, Crit. Care 18 (2) (2014) R52. [PubMed: 24666991]

[37]. Hayakawa M, Dynamics of fibrinogen in acute phases of trauma, J. Intens. Care 5 (1) (2017) 3.

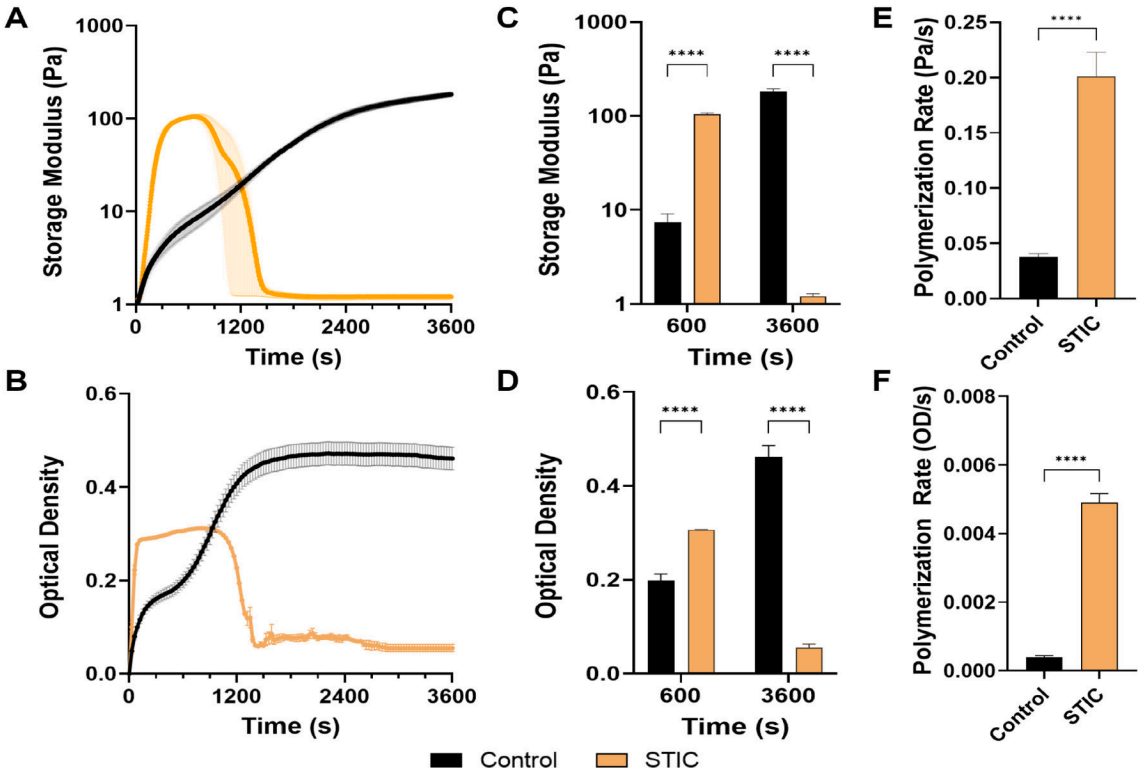

Fig. 1.

Mechanical and Optical Analysis of STIC Clotting.

Clot formation profile in control and simulated Trauma Induced Coagulopathy (STIC) PPP samples after activation assessed by (A) rheometer and (B) optical turbidity testing. Sample composition described in Table 2, STIC samples contain 45 pM TF, 3.3 mM tPA, and 15 % dilution with saline in addition to the control sample. Comparison of two time points during the plasma clotting formation profile from (C) rheometer and (D) optical turbidity testing. Fibrin polymerization rate taken from 1 to 40 % during the clotting profile for (E) rheometer and 20 to 70 % during (F) optical turbidity testing. * $p \leq 0.05$, ** $p \leq 0.01$, *** $p \leq 0.005$, **** $p \leq 0.001$. ($n \geq 3$ for all samples).

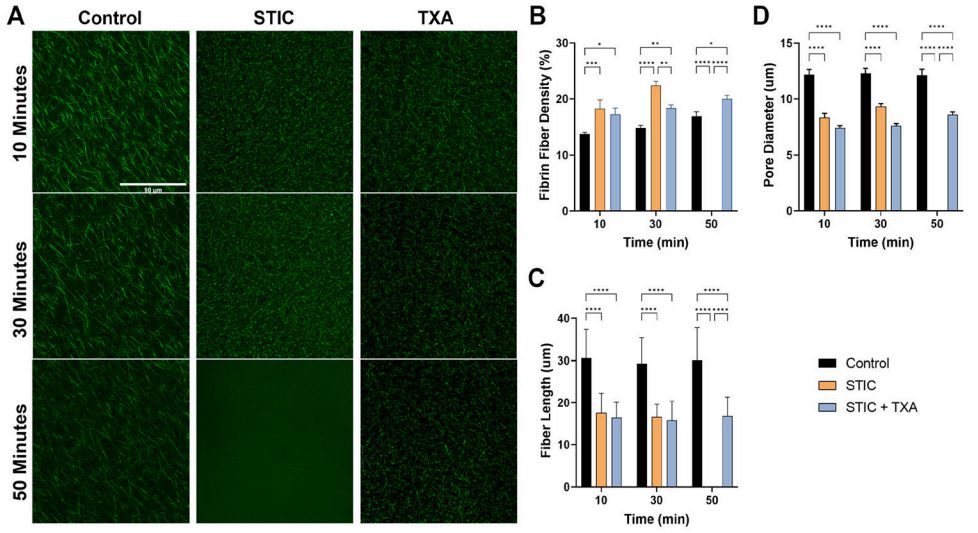

Fig. 2.

Confocal Images of Control, STIC and STIC + TXA Clots.

(A) Confocal images of Control, STIC, and STIC+TXA plasma with 1 % (%*v*/v) 1.5 mg/mL Alexa Fluor 488 fluorescent fibrinogen. (B) Fibrin fiber density, (C) fiber length and (D) pore size from confocal analysis. No fibers present after 30 min in STIC sample. Scale bar = 90 um. * $p \leq 0.05$, ** $p \leq 0.01$, *** $p \leq 0.005$, **** $p \leq 0.001$. (n = 3 for all samples).

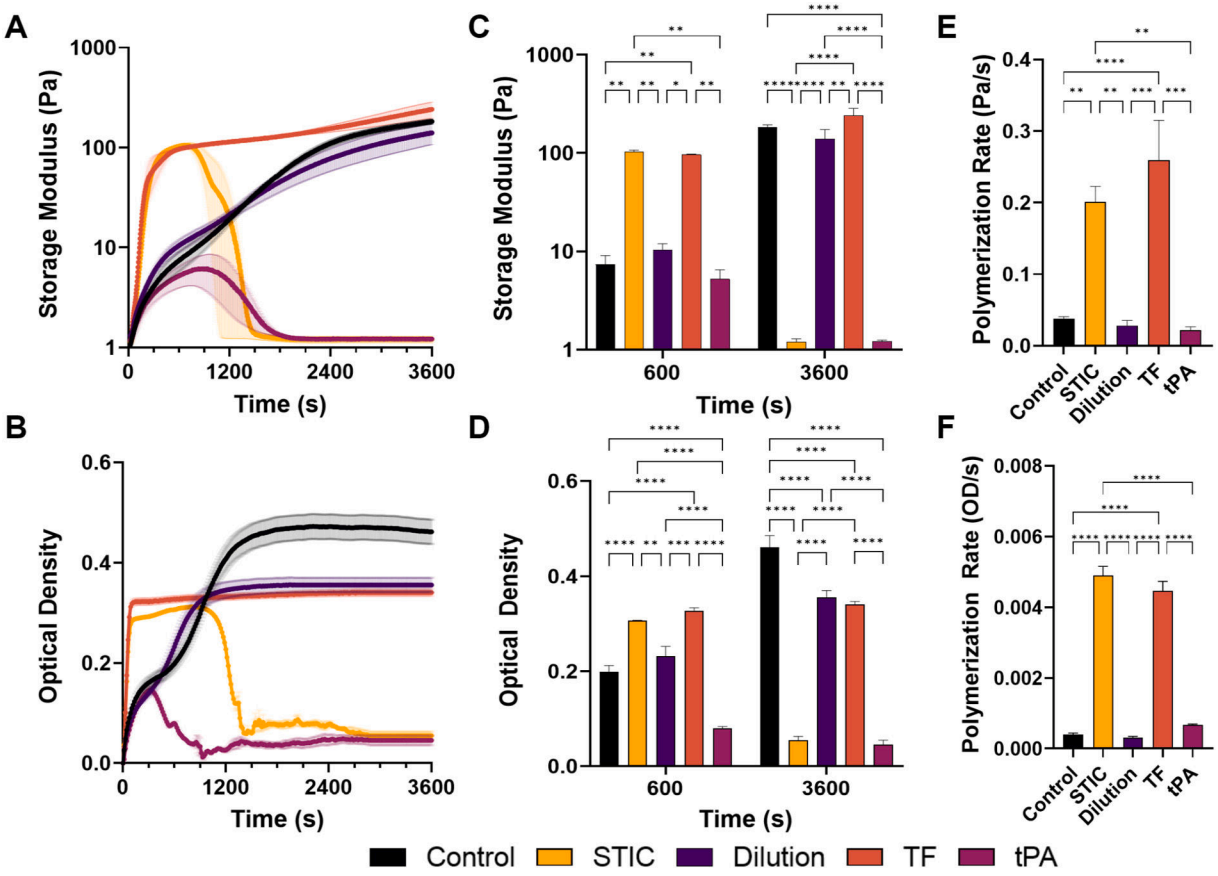

Fig. 3.

Mechanical and Optical Analysis of STIC and Components on Plasma Clotting.

Clot formation profile in PPP control, simulated Trauma Induced Coagulopathy (STIC) and PPP supplemented with individual STIC component, 15 % saline dilution, 3.3 mM tPA, and 45pM TF after activation assessed by (A) rheometer and (B) optical turbidity testing. Sample composition described in Table 2. Comparison of (C) storage modulus and (D) optical density at two time points after clot activation. Fibrin polymerization rate taken from 1 to 40 % during the clotting profile for (E) rheometer and 20 to 70 % during (F) optical turbidity testing. *$p \leq 0.05$, ** $p \leq 0.01$, *** $p \leq 0.005$, **** $p \leq 0.001$. ($n \geq 3$ for all samples).

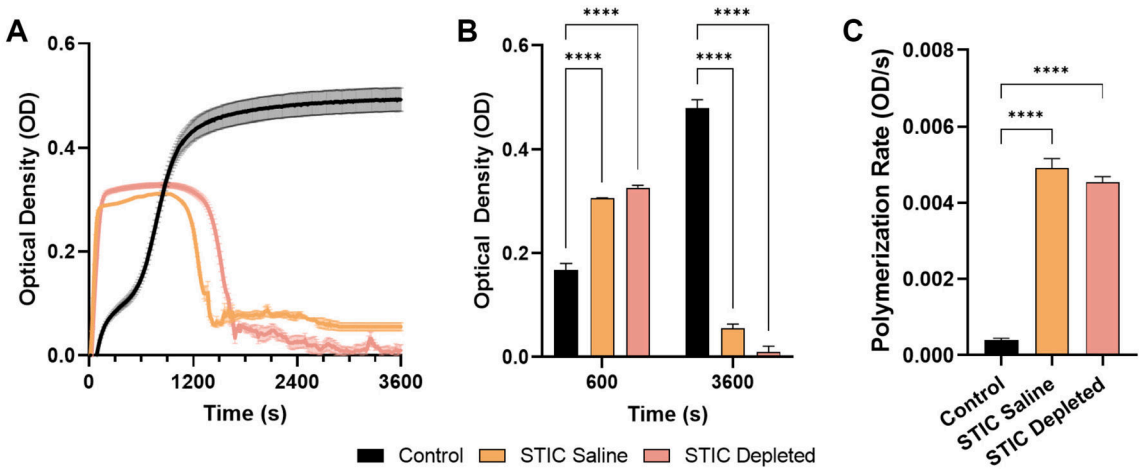

Fig. 4.

Impact of Fibrinogen Consumption on Plasma Clot and STIC Optical Turbidity.

Clot formation profile in PPP control, simulated Trauma Induced Coagulopathy (STIC) diluted with saline, and fibrinogen depleted plasma after activation assessed by (A) optical turbidity testing. (B) Comparison of discrete time points assessing differences between STIC diluted with fibrinogen depleted plasma or saline, and controls. (C) Fibrin polymerization rate taken from 20 to 70 % during the clotting profile for optical turbidity testing. **** $p \leq 0.001$. ($n \geq 3$ for all samples).

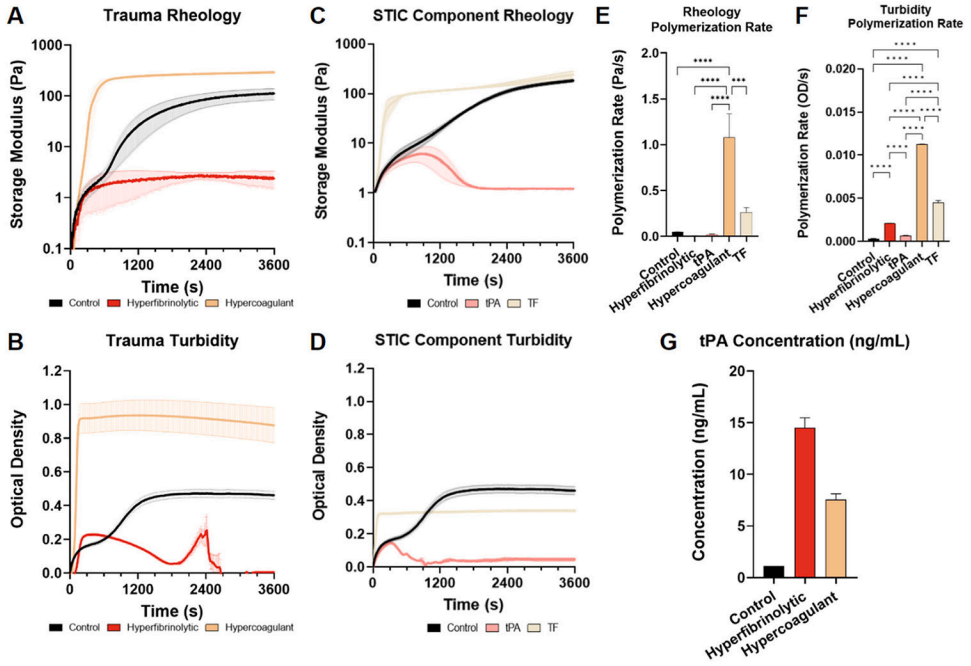

Fig. 5.

Comparison of Trauma Patient Coagulation Profiles and STIC Component Samples

Clot formation profile of trauma patient platelet poor plasma during coagulation after activation with 0.2 U/mL thrombin and 20 mM $CaCl_2$ in (A) mechanical testing and (B) optical turbidity testing. Clot formation profile of pooled platelet poor plasma supplemented with 3.3 mM tPA or 45pM TF after activation with 0.2 U/mL thrombin and 20 mM $CaCl_2$ in (C) mechanical testing and (D) optical turbidity testing. Fibrin polymerization rate comparison in (E) rheometry and (F) optical turbidity testing. (G) Tissue plasminogen activator concentration determined by ELISA, indicating higher tPA concentration associated with increased lysis. *Lack of significance indicated by no bar above data, *** $p \leq 0.005$, **** $p \leq 0.001$ ($n \geq 2$ for all samples).*

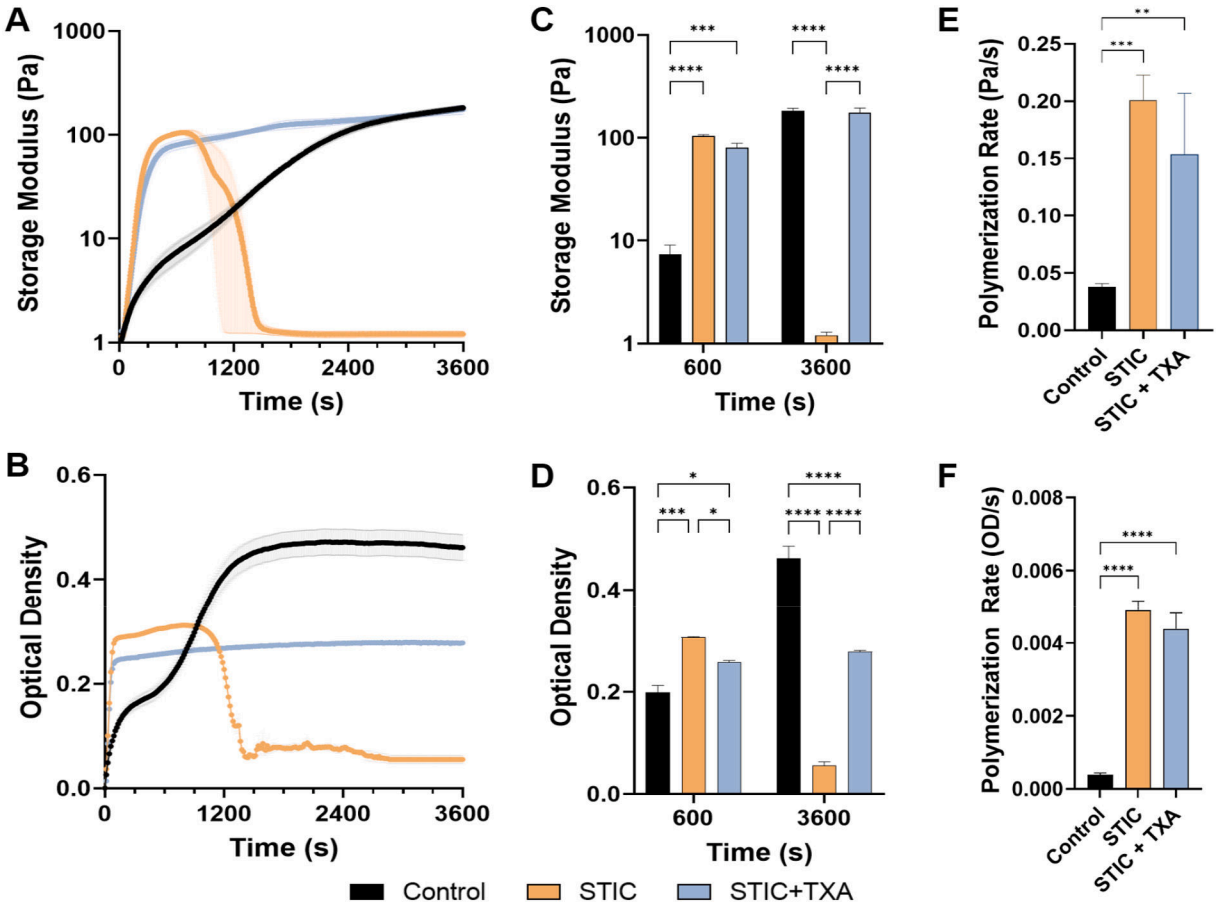

Fig. 6.

Tranexamic Acid (TXA) Administration Impact on STIC Clot Lysis.

Clot formation profile in platelet poor plasma comparing impact of TXA administration in STIC clots in (A) rheometer and (B) optical turbidity testing. Comparison of discrete time points assessing impact of TXA addition on plasma clotting from (C) rheometer and (D) optical turbidity testing. Fibrin polymerization rate taken from 1 to 40 % during the clotting profile for (E) rheometer and 20 to 70 % during (F) optical turbidity testing. *$p \leq 0.05$, ** $p \leq 0.01$, *** $p \leq 0.005$, **** $p \leq 0.001$. ($n \geq 3$ for all samples).

Table 1

Patient demographics and clinical parameters.

Patient characteristics		
Coagulation phenotype	**Hyperfibrinolytic**	**Hypercoagulant**
Patient number	Patient #1	Patient #2
Age	23	59
Sex	Male	Female
Race	Black	Black
Ethnicity	Not Hispanic or Latino	Not Hispanic or Latino
Mechanism of Injury	Gunshot Wound	Motor Vehicle Collision
In hospital mortality	Yes	No
Trauma scores		
Glasgow coma scale	3	15
Injury severity score	75	32
Labs		
Hemoglobin [g/dL]	9.7	13.2
Platelet Ct [10^3/uL]	81	312
WBC Count [10^3/uL]	31.5	23
RBC Count [10^3/uL]	3.49	4
PTT [*sec*]	112	25
PT [*sec*]	22.3	11.9
INR	1.98	1.06
D-Dimer [ng/mL]	128,000	7370
Fibrinogen [mg/dL]	38	448
Blood Products in 24 h [units]		
Packed red blood cells	2	1
Fresh frozen plasma	2	0
Platelets	0	0
Cryoprecipitate	0	0

Table 2

Composition of plasma samples tested.

Sample	FBG[a] (mg/mL)	Plasma (%v/v)	Saline (%v/v)	FDP (%v/v)	tPA (mM)	TF (pM)	TXA (mM)	$CaCl_2$ (mM)	Thrombin (U/mL)
Control	2.70	100	0	0	0	0	0	20	0.2
STIC[b]	2.30	85	15	0	3.3	45	0	20	0.2
Depleted STIC	2.30	85	0	15	3.3	45	0	20	0.2
STIC + TXA[c]	2.30	85	15	0	3.3	45	10	20	0.2
15 % Saline	2.30	85	15	0	0	0	0	20	0.2
30 % Saline	1.89	70	30	0	0	0	0	20	0.2
45 % Saline	1.49	55	45	0	0	0	0	20	0.2
60 % Saline	1.08	40	60	0	0	0	0	20	0.2
15 % FDP[d]	2.30	85	0	15	0	0	0	20	0.2
30 % FDP	1.89	70	0	30	0	0	0	20	0.2
45 % FDP	1.49	55	0	45	0	0	0	20	0.2
60 % FDP	1.08	40	0	60	0	0	0	20	0.2
tPA[e]	2.70	100	0	0	3.3	0	0	20	0.2
2× tPA	2.70	100	0	0	6.6	0	0	20	0.2
TF[f]	2.70	100	0	0	0	45	0	20	0.2
2× TF	2.70	100	0	0	0	90	0	20	0.2
STIC + TXA no tPA	2.30	85	15	0	0	45	10	20	0.2

[a] Fibrinogen (FBG).

[b] Simulated Trauma Induced Coagulopathy (STIC).

[c] Tranexamic Acid (TXA).

[d] Fibrinogen Depleted Plasma (FDP).

[e] Tissue Plasminogen Activator (tPA).

[f] Tissue Factor (TF).